Alexandria Journal of Science and Technology

Article

Evaluation of Geothermal Energy Potentiality in the Junction between the Red Sea and the Gulf of Suez, Egypt

Maria G. Kayser [*] , Ahmed M. Bekhit , Tharwat A. Abdel Fattah

Geology Department, Faculty of Science, Alexandria University, Alexandria, Egypt.

[*] *Correspondence Address:*

Maria G. Kayser: Geology Department, Faculty of Science, Alexandria University, Alexandria, Egypt. Email address: mariakayser2001@gmail.com.

KEYWORDS: Geothermal, Curie, Red Sea, Gulf of Suez.

Received:
October 07, 2024
Accepted:
February 21, 2025
Published:
June 03, 2025

ABSTRACT: Egypt has a range of renewable energy sources. Our main purpose of this research is to extend our study of the potentiality of geothermal resources in Egypt to be used as a primary energy source in the future, especially in the southern Gulf of Suez. Gravity, magnetic, and well logs, as well as interpolating basement depth from the wells, are used to detect the potentiality of the geothermal energy. A temperature grid from wells was created, and a 3D cube was established to show the relation between temperature increase and depth using Geosoft Oasis Montaj and Python software. We revealed the subsurface geology and tectonics of the study area, which led to identify the main reason and source for geothermal energy and the relationships between different data sets and the existence of geothermal energy. By calculating the geothermal gradient along various depths and assessing the discrepancies between different geophysical models, our investigation revealed that the depth to the basement did not yield significant results, likely due to the complex geological structure of the study area. However, by analyzing the Moho and Curie depths, we discovered a temperature gradient that increases toward the northern region. We established a relationship among bottom hole temperature (BHT), basement depth, Moho depth, and Curie depth to accurately identify areas of interest for drilling. This analysis enabled us to select the most promising location for geothermal potential, situated in the northern section of the study area at an approximate depth of 2,550 meters.

1. INTRODCTION

Because global energy consumption is increasing and fossil fuels such as coal, petroleum, and natural gas are no longer the primary energy sources, the current trend is to meet energy demands with cleaner and more environmentally friendly resources such as geothermal energy. This is because geothermal energy has a significantly higher capacity than other forms of renewable energy, so it is continuous rather than intermittent. Luckily, Egypt has a considerable number of geothermal resources due to its location in the northern east corner of Africa with an active rifting in the red sea, Gulf of Suez and Gulf of Aqaba region which form the extension of the east African rift system [1].

To identify potential geothermal reservoirs, we utilized descriptions from previous research about Egypt's subsurface geological structure. Drawing on findings from earlier studies that employed a range of methods including gravity, magnetic, and seismic analyses, as well as remote sensing and satellite imagery, we have enhanced our understanding of the geological framework crucial for geothermal exploration. The dynamics of Egypt's lithosphere are influenced by the movements of three significant tectonic plates: Africa, Arabia, and Eurasia, which contribute to a complex geodynamic landscape [2].

Recent work by [3] estimated Egypt's crustal thickness using inverse and forward gravity modeling, finding values ranging from 15 to 45 kilometers, [4] explored the crustal thickness and structural features of the Sinai Peninsula through 3D density modeling, integrating aeromagnetic and seismic data. Furthermore, [5] developed 3D structural models for the Conrad and Moho discontinuities across different tectonic regions in Egypt.

The study area, lies in the southeastern part of the Gulf of Suez,

Alexandria Journal of Science and Technology, 2025, **3**(1), 82–90
Online ISSN: 2974-3273

DOI: 10.21608/AJST.2025.326547.1048

between latitude 26º and 29ºN and longitude 32º and 35ºE (**Figure 1A**), representing a rift area characterized by an extensional half-graben structure dominated by normal faults and a deep graben-bounding master fault (**Figure 1B**). Notably, deep faults are crucial in controlling fluid flow and heat transport in geothermal systems, making them a key aspect in understanding Egypt's geothermal potential [6].

1.1.Geological Background

The study area, located in the Gulf of Suez. It is a failed rift, a product of the Aqaba-Dead Sea transform fault's emergence and a rapid surge in extension rates during the peak of extension 20 million years ago [7]. The region's formation was also influenced by a triple junction and tensional forces, which have sculpted its unique landscape. These exceptional geological characteristics make the Gulf of Suez an intriguing focus of study [7,8,9,10]. The Gulf of Suez is far from a straightforward geological entity. It is a region composed of numerous blocks that have undergone continuous uplift and subsidence at different times and with varying magnitudes and intensities. The succession, facies changes, and relationships of these blocks are so diverse that no single area in the Gulf can fully represent the stratigraphy or the structure of the entire region. This intricate web of the Gulf's geological history presents a fascinating and intellectually stimulating challenge for researchers [1].

The Gulf of Suez is one of the most geologically active areas on Earth. Two large marginal faults that border the depression on both sides are responsible for separating the heavily disturbed gulf region from the fairly undisturbed massifs of central Sinai and the central plateau of the Eastern Desert; these faults are typically identified by lines of high vertical escarpments on the up thrown sides. These two main lines of fracture largely determine the current Gulf's structure. Folding was also a significant factor in establishing the structure of the Gulf; all of the folds that were observed were either formed by movements that led the less rigid sediments (particularly the Miocene) to bend in anticlinal or synclinal folds, or by the strata bending before breaking. The Gulf's stratigraphic sequence in various locations suggests that the movements were not constant in size across the Gulf, and several of the blocks display varying activity levels on their various sides. The Gulf of Suez region's history can be understood as the rising and falling of numerous blocks that form or border the Gulf of Suez. While some of these blocks, like Raha, northern Galala, and Ataqa are splinter blocks that appear to be newer, others have substantial proportions and have been active since early geological time. From middle cretaceous to Oligocene, the blocks were particularly active. Most of the blocks appear to have been impacted by the migration toward the end of the lower Eocene or the beginning of the middle Eocene, and evidence suggests that this is when the Sinai massif and Red Sea ranges began to separate [11].

The stratigraphic succession in the southern Gulf of Suez is divided into three major mega units: pre-rift, syn-rift, and post-rift sediments. The pre-rift sediments consist of older geological formations, such as the Khatatba Formation and the Rudeis Formation, which were deposited before the onset of rifting and are characterized by marine deposits. The syn-rift sediments, formed during the rifting process, include the Nukhul Formation, comprising mainly clastic sediments with significant shale components; the Rudies Formation, distinguished by alternating layers of sandstones and shales indicative of a fluctuating depositional environment; the Kareem Formation, known for its carbonate and clastic deposits representing shallow marine conditions; the Belayim Equivalent, featuring fine-grained sediments that are crucial for understanding the hydrocarbon potential of the region; the South Gharib Formation, which displays a mixture of clastics and carbonates reflecting diverse depositional settings; and the Zeit Formation, the youngest syn-rift unit primarily composed of sandstones and shales, marking the transition to post-rift conditions. These formations are essential for elucidating the sedimentary environments and hydrocarbon potential of the Gulf of Suez. Finally, post-rift sediments, deposited after the rifting has ceased, include notable units such as the Bahr El-Baqar Formation and the Miocene and Pliocene sediments, which contain significant hydrocarbon reservoirs. This comprehensive stratigraphic framework is vital for hydrocarbon exploration and for understanding the geological history of the Gulf of Suez [12, 1].

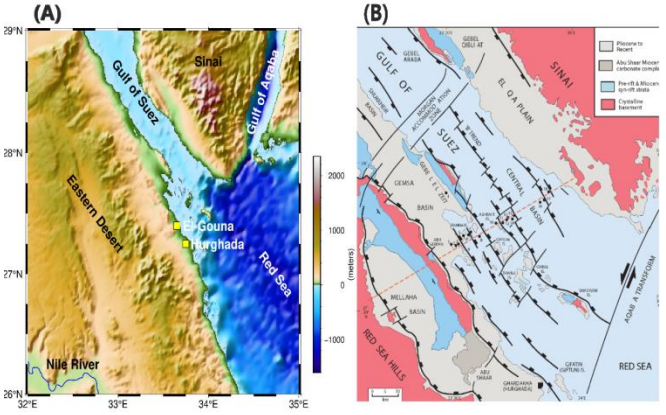

Figure 1. (A) Digital Elevation map of the study region, and (B) Tectonic map of the study region, modified after [13].

2. Results and Discussion

Bottom Hole Temperature (BHT) measurements were collected from 44 wells and complied into eight isothermal layers, spanning depths from 1085.5 m to 3877.66 m (**Figure 2**). The first layer, starting at 1085.5 m, included wells 30–38, with an average temperature of 78°C. The second layer, at 1235 m, encompassed wells 2, 6, 8, and 30, recording an average temperature of 77.41°C. The third layer, located at 1348.63 m, comprised wells 3, 5, 9, 13, 15, and 37, with an average temperature of 81.88°C. The fourth layer, at 1676.5 m, included wells 7, 20, 23, 32, 40, 41, 10, and 12, recording a temperature of 82.3°C. The fifth layer, at 2097.39 m, included wells 33, 34, 35, 36, and 43, with a temperature of 98.77°C. The sixth layer, at 3044.36 m, comprised wells 39 and 22, with a recorded temperature of 119.4°C. The seventh layer, also at 3044.36 m, included wells 21, 24, 17, 28, and 29, which had an average temperature of 122.67°C. Finally, the eighth layer, reaching 3877.66 m, included wells 31, 18, and 19, recording a temperature of 141.34°C.

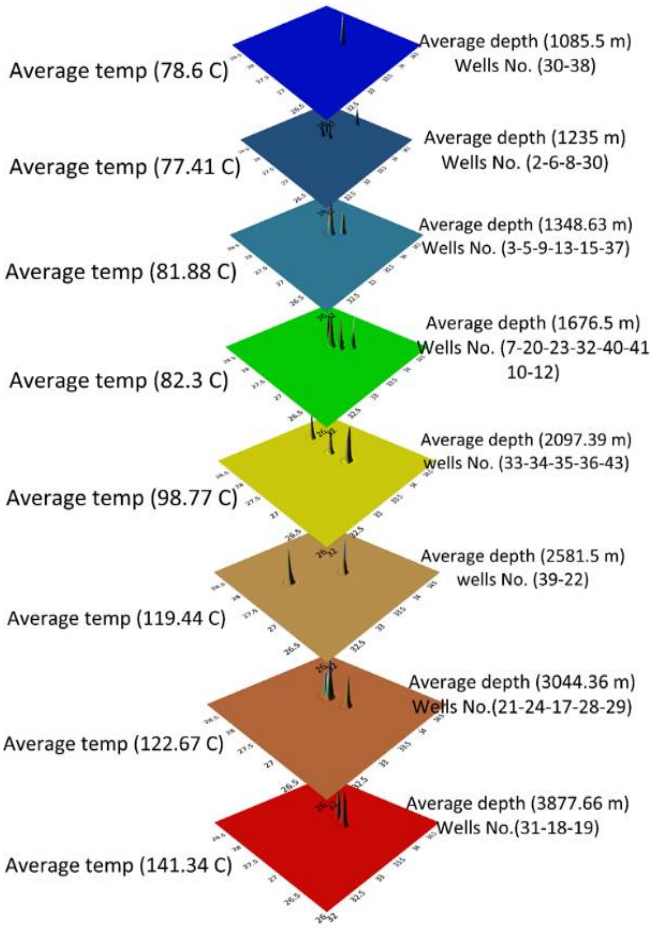

Figure 2. The isothermal slices of each group of wells.

Subsequent analysis of the BHT-depth relationship facilitated the computation of geothermal gradients for each interval. The geothermal gradient was calculated as follows: -0.79°C/100 m for the first interval (1085.5–1235 m), 3.93°C/100 m for the second interval (1235–1348.63 m), 0.12°C/100 m for the third interval (1348.63–1676.5 m), 3.91°C/100 m for the fourth interval (1676.5–2097.3 9 m), 4.26°C/100 m for the fifth interval (2097.39–2581.5 m), 0.69°C/100 m for the sixth interval (2581.5–3044.36 m), and 2.24°C/100 m for the seventh and eighth intervals (3044.36–3877.66 m). As illustrated in Table 1 and **Figure 3**, the fourth and fifth intervals exhibited the highest geothermal gradients, indicating enhanced geothermal potential at depths between 1676.5 m and 2581.5 m.

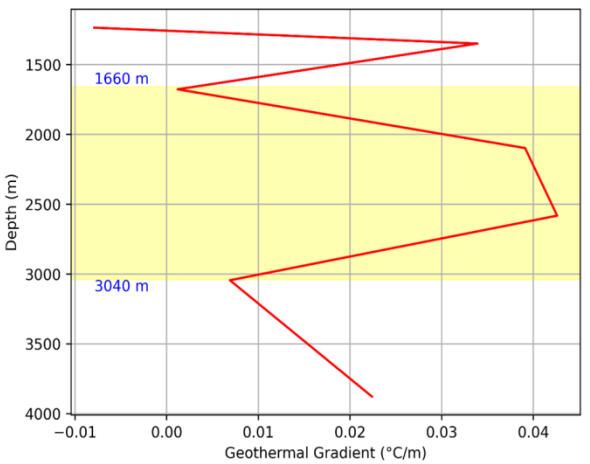

Figure 3. A graph shows the geothermal gradient variations with depth.

Table 1. The temperature gradient with depth; the highest geothermal intervals are highlighted in green.

Depth (m)	Depth difference (m)	BHT (°C)	Geothermal Gradient (°C/m)	Geothermal Gradient (°C/100 m)
1085.5 – 1235	149.5	78.6 – 77.41	-0.0079	-0.79
1235 - 1348.63	113.63	77.41 – 81.88	0.0393	3.93
1348.63 - 1676.5	327.87	81.88 – 82.3	0.0012	0.12
1676.5 - 2097.39	420.89	82.3 – 98.77	0.0391	3.91
2097.39 - 2581.5	484.11	98.77 – 119.44	0.0426	4.26
2581.5 - 3044.36	462.86	119.44 – 122.67	0.0069	0.69
3044.36 - 3877.66	833.3	122.67 – 141.34	0.0224	2.24
1085.5 – 3877.66	2792.16	78.6 -141.34	0.0224	2.24

Misfit analyses between the well BHTs and subsurface structural models revealed no significant correlation with the depth to basement, likely due to the region's complex tectonic fabric. In contrast (**Figure 4A**), a strong spatial relationship was observed between BHT and Curie depth (ranging from 10 to 35 km), with temperatures increasing towards the northern portion of the study area. Conversely (**Figure 4B**), the Moho depth (ranging from 25 to 40 km) showed increasing temperatures towards the southeastern sector, associated with crustal thinning and density anomalies related to the Red Sea Rift (**Figure 4C**). Given that Curie depth is less influenced by gravitational anomalies compared to Moho depth, it was deemed a more reliable indicator of subsurface thermal structure.

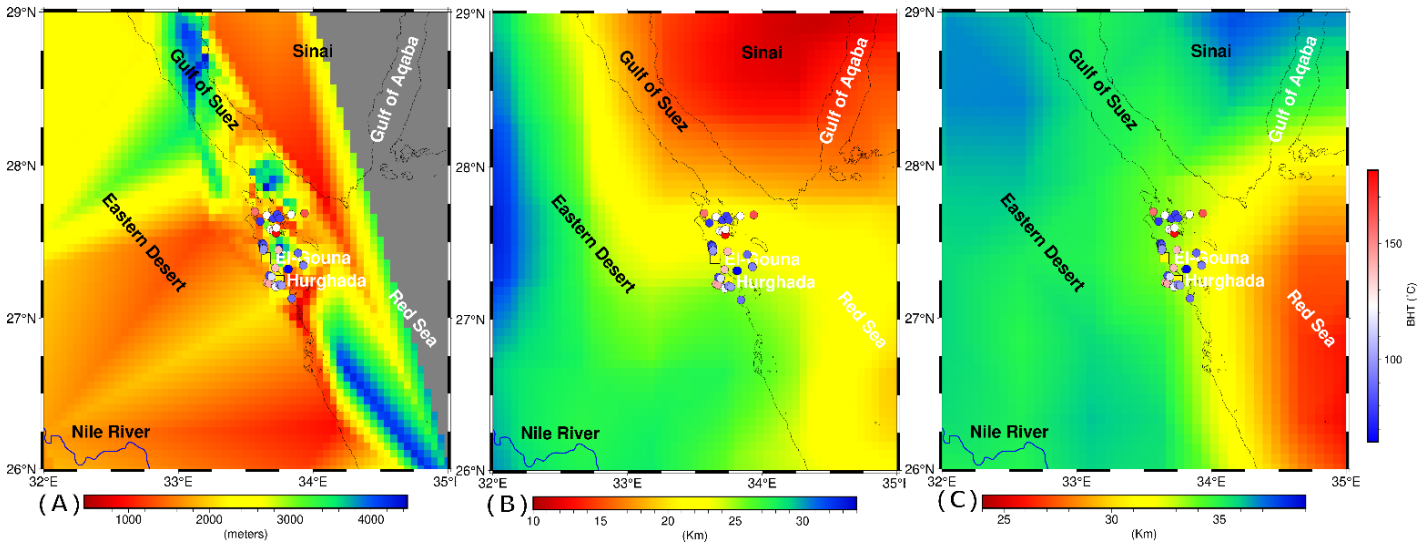

Figure 4. Relation between BHT and (A) basement depth, (B) Curie depth and (C) Moho depth.

A three-dimensional integrated model, constructed using Surfer software, combined BHT, basement depth, Curie depth, and Moho depth, allowing for more precise delineation of prospective geothermal zones. The analysis revealed BHT between 75°C and 155°C (**Figure 5A**), while variations in basement depth could not be reliably interpreted due to structural complexities, fluctuated between 0.2 to 4.2 km (**Figure 4B**). Moho depths between 25 and 37 km (**Figure 4C**), and Curie temperature depths values ranging from 10 to 35 km (**Figure 4D**).

This study has emphasized the southern Gulf of Suez's substantial and underutilized geothermal potential, focusing on the Hurghada region, positioning it as a promising area for renewable energy development in Egypt's energy transition strategy. The analysis of Bottom Hole Temperature (BHT) data from well measurements reveals a consistent increase in temperature with depth, ranging from approximately 78°C at 1,085.5 Meters depth to 141.34°C at 3,877 meters depth. Although the overall trend is upward, the temperature-depth relationship is not strictly linear. This nonlinearity reflects a complex interplay of subsurface geological factors, including lithological variations, differences in rock thermal conductivity, and the movement of geothermal fluids along the fault and fracture zones. A more rapid temperature increase was recorded between 2,000 and 3,000 Meters depth, pointing to localized zones of enhanced heat flow likely associated with structural influences, such as fault-controlled convection or conductive heat anomalies in fractured rocks. The observed variations in BHT with depth across the Hurghada area can be directly attributed to two dominant geological controls: the region's elevated geothermal gradient and its tectonic-structural framework. The geothermal gradient in the southern Gulf of Suez is significantly higher than those found in tectonically stable continental interiors. This elevated gradient results from the rifting events that have shaped the Gulf of Suez since the Oligocene–Miocene, leading to regional crustal thinning and extensional deformation. As the continental lithosphere becomes stretched and thinned, it allows for more efficient heat transfer from the underlying asthenosphere toward the surface. Geothermal gradients commonly range between 25°C and 35°C/km in such rift settings. However, depending on local geology, sediment accumulation rates, and heat conductivity properties, they can reach even higher values in fault-dominated zones. These conditions are further amplified by the presence of deep-seated faults that act as conduits for thermal fluids, effectively creating vertical heat transport pathways and enhancing localized geothermal anomalies [14,15].

In the Hurghada region, these tectonic and structural characteristics are particularly well-developed. The combination of deep faulting, crustal thinning, and magmatic activity associated with rifting contributes to significant variations in subsurface temperature regimes. The stratigraphic intervals known as the fourth and fifth layers show particularly high geothermal gradients, reaching values up to 4.26°C per 100 meters. These layers, located roughly between 1,660 and 3,040 meters in depth—with a notable thermal peak at approximately 2,550 meters—have been identified as prime targets for geothermal energy extraction. The thermal characteristics at these depths make them ideal zones for future drilling and geothermal exploitation, as they promise high energy yields with relatively manageable drilling depths and costs. Moreover, this study integrates and correlates multiple geophysical and geological datasets—including well logs, magnetic surveys, and gravity data—to comprehensively understand the subsurface conditions. This integrative approach revealed a strong and meaningful correlation between three critical geothermal indicators: geothermal gradient, Curie point depth (CPD), and BHT. Curie point depth, which marks the boundary in the crust below which rocks lose their permanent magnetism due to high temperatures (around 580°C), is an important proxy for assessing regional heat flow. In the Hurghada area, CPD values are relatively shallow, indicating elevated heat flow consistent with the rifted nature of the Gulf of Suez. These shallow CPDs align spatially with areas of high geothermal gradient and elevated BHT, reinforcing the reliability of these indicators in identifying zones of geothermal potential [16].

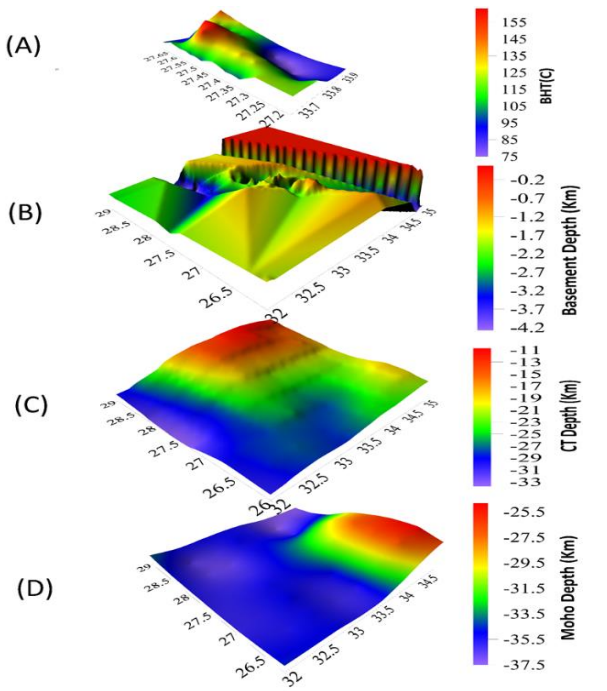

Figure 5. (A) BHT, B) Basement depth, (C) CT depth, and (D) Moho depth respectively as slices.

The northward increase in geothermal gradient and Curie depth across the study area further supports the hypothesis of a spatially varying geothermal regime influenced by tectonic segmentation and crustal heterogeneities. Despite complex geological structures that occasionally obscure the precise interpretation of basement and Moho depths, regional gravity data suggest an increase in Moho depth southward, possibly due to lower crustal density. This variation adds another layer of complexity but also offers clues about the broader rift system's thermal structure and tectonic evolution. Notably, this density contrast and resulting crustal geometry help explaining the variations in heat flow and may further inform future geothermal exploration models.

The implications of this research extend beyond the realm of academic inquiry and into the strategic planning of Egypt's energy future. With increasing national and global emphasis on clean, renewable energy sources, geothermal energy represents a largely untapped opportunity for Egypt, particularly in tectonically active regions such as the Gulf of Suez. Egypt can move toward a more sustainable and resilient energy infrastructure by integrating geothermal energy into the broader energy mix—alongside solar, wind, and potentially offshore energy resources. Reducing reliance on fossil fuels supports environmental goals and strengthens national energy security by diversifying energy sources and reducing vulnerability to global energy market fluctuations.

In summary, this study identifies the Hurghada region in the southern Gulf of Suez as a key geothermal hotspot with strong scientific and economic justification for further exploration. The convergence of high geothermal gradients, shallow Curie depths, and elevated BHT values—all driven by active tectonics and crustal thinning-marks this area as a high-potential zone for geothermal energy development. Future efforts, including exploratory drilling and pilot geothermal projects, could unlock Egypt's vital new energy resource, supporting long-term sustainability and energy independence.

3. Material and Methods

3.1. Material and Processing

3.1.1. Topography Data

We utilized topography data from ETOPO1 model, a 1 arc-minute global relief model of Earth's surface that combines land topography and ocean bathymetry. It was developed using multiple global and regional data sets and is accessible in "Ice Surface" (top of Antarctic and Greenland ice sheets) and "Bedrock" (base of ice sheets) versions [17]. The area of study is the Gulf of Suez which is a part of Red sea that penetrates land between Sinai and Eastern Desert (**Figure 1A**).

3.1.2. Gravity Data

We obtained gravity data from XGM2019e model; a global gravity field model with spheroidal harmonics up to degree and order (d/o) 5399. This corresponds to a spatial resolution of 2′ (~4 km). XGM2019e is composed of three main data sources: the combined satellite-only model GOCO06s, the 15′ ground gravity anomaly dataset provided by NGA, and the 1′ min augmentation dataset consisting of gravity anomalies derived from altimetry over the oceans and topography over the continents. It includes the satellite model GOCO06s in the longer wavelength range up to d/o 300, as well as a ground gravity grid that covers the shorter wavelengths [18]. From the raw gravity map of the area (**Figure 6A**), we observed a local increase in gravity anomaly in the northern trend and decreases southward.

3.1.2.1. Processing of Gravity Data

During the processing step, we used an open-source code [19] to calculate gravity disturbance, then topography was corrected for gravity disturbance using the etopo1 and crust1 models, the Moho depth is determined by CRUST01 model based on 1-degree averages of a recently updated database of crustal thickness data from receiver function studies and active source seismic studies. Gravity constraints are used to estimate crustal thicknesses in regions where such constraints are still absent [20,17].

Finally, the Bouguer anomaly and Moho effect were distinguished by removing gravitational influence from sedimentary layers, **(Figure 6B)** The final processed map looks to have a range of (-5 to 70 mGal), with the highest value inside the Red Sea rift due to the thin and deep crust so its density increases as the temperature increases, and decreasing to the Eastern Desert and Sinai Peninsula.

3.1.3. Moho Depth

Moho is the boundary separating the mantle from the crust of the Earth. The Moho is located roughly 4.5 miles (7 km) below the oceanic crust and 22 miles (35 km) below continents. At this barrier, seismic wave velocity increases rapidly, as measured by modern sensors [21,18]. We employed the Moho depth model of [3], and the Moho depth of the area fluctuates between 24 km in the Red Sea Rift to 38 km in Sinai and Eastern Desert. This indicates that the thinnest crustal zone in the area is located within the Red Sea, south of the Gulf of Suez (**Figure 6C**).

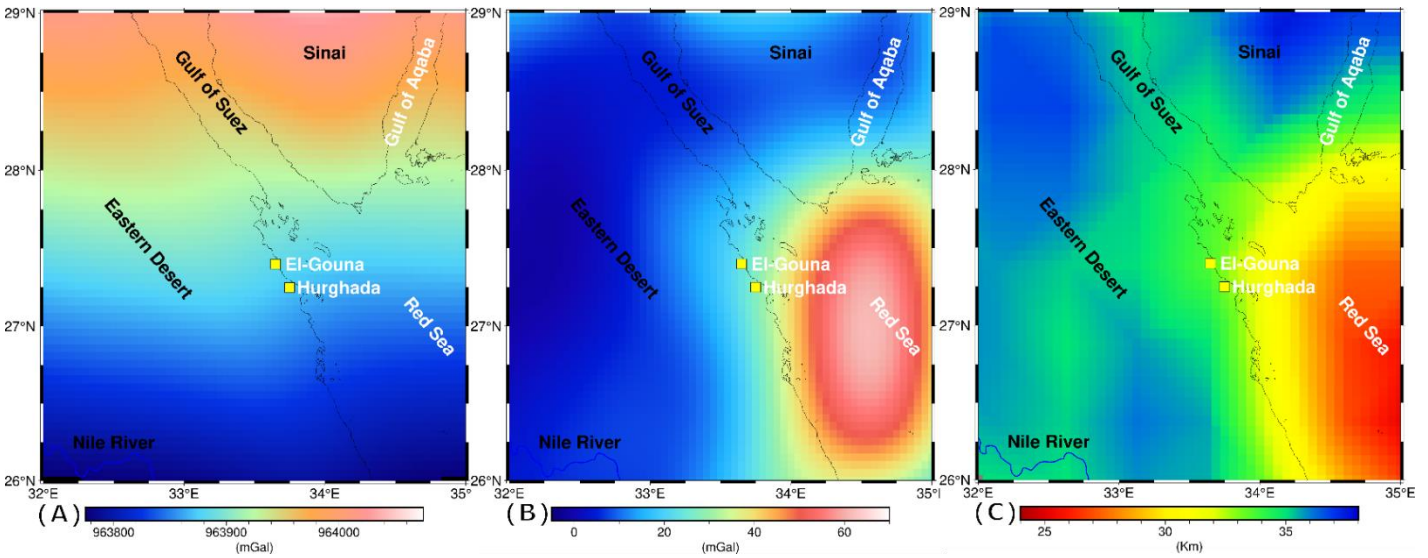

Figure 6. (A) Raw satellite gravity based on XGM2019e [22], (B) Processed gravity, and (C) Moho depth map [3].

3.1.4. Magnetic Data

We gathered the magnetic data of the study area using the EMAG2 model [22], a global Earth magnetic anomaly grid comprised of satellite, ship, and airborne magnetic measurements. It is a significant update to the Earth Magnetic Anomaly Grid's previous release (**Figure 7A**). The resolution remains 2 arc-minutes. The altitude of 4 km above the geoid is still supported but an additional product. This grid is observed at sea level over oceanic regions; from the magnetic map of the study area, we observed a gradual increase in the values from 50 to 100 nT in the northern part of the Red Sea.

3.1.5. Curie Depth

The Curie depth, a key concept in our research, is the depth at which the rock achieves the curie temperature and loses all magnetic properties. This depth is of significant importance in geothermal exploration, as it helps us understand the thermal structure of the Earth's crust. With the recent advancements in the global coverage of magnetic anomalies, we can now map the global Curie isotherm in high resolution, assuming a constant Curie-point temperature globally at 550°C and negligible lateral changes in composition's impact on the Curie temperature [23]. We eventually created a map showing the link between magnetic anomaly and Curie temperature depth (**Figure 7B**), and from that, we observed a severe increase in the Curie depth northward of the map.

3.1.6. Well Data

3.1.6.1. Basement Depth Wells

We collected 140 basement wells with their total depth and BHT values (**Figure 8A**) [24], then we interpolated the values and created a model that displayed the depth to the basement of the area, the map on the right-hand side (**Figure 8B**) did not give a clear deduction on the depth to basement of the area due to the complex structure of the Gulf of Suez and red sea failed rift as long as the tens of minor faults that affected the resolution of the final output data.

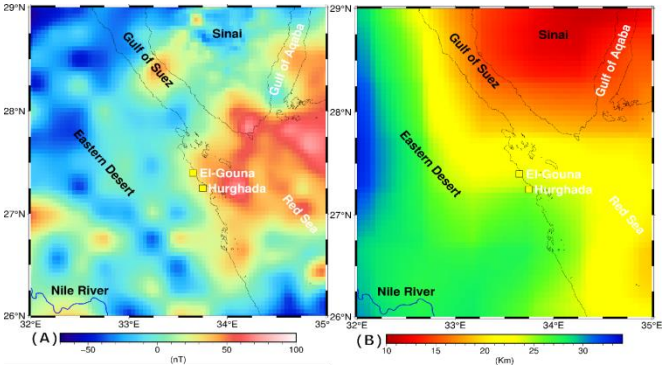

Figure 7. (A) Aeromagnetic data compiled from EMAG2 global model [22], (B) Curie depth derived from [23].

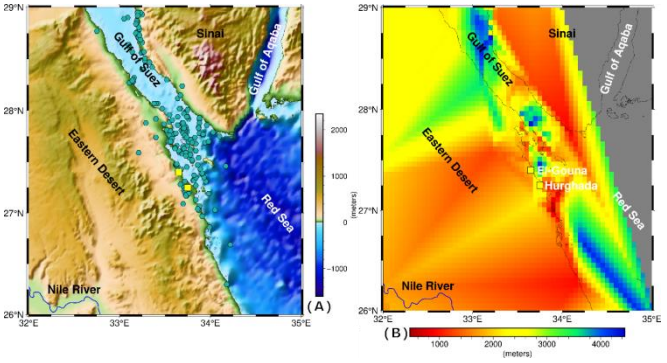

Figure 8. (A) DEM shows the location of basement wells represented by Cian hexagons, and (B) the depth to basement interpolated from A.

3.1.6.2. Temperature Wells

We obtained both temperature log data using 44 offshore and onshore drilled wells located within the study area, they were drilled by oil firms including the Egyptian General Petroleum Company (EGPC), the Gulf of Suez Petroleum Company (GUPCO), and the British Petroleum Company (BPC), with depths ranging from 950 to 4500 meters (**Figures 9A&B**).

3.1.6.2.1. Correction of Temperature Wells

The actual borehole temperature is greater than the recorded temperature because mud is used during the circulation to stabilize the borehole so it decreases the actual temperature. The adjustments were made using an empirical method developed by [25] and applied to our data as shown in **(Figures 9A, B)**, and (Table 2).

Table 2. The BHT wells after correction [13].

no	Well Name	Latitude	Longitude	BHT(°C)	Depth (m)	no	Well Name	Latitude	Longitude	BHT(°C)	Depth (m)	no	Well Name	Latitude	Longitude	BHT(°C)	Depth (m)
1	RR-89	27.70	33.57	155.61	2484.00	16	EEMM-23	27.45	33.63	98.00	1424.03	31	Abu-Shaar-NE-1	27.45	33.74	138.56	4524.76
2	Gabrit-Pass-1	27.64	33.61	76.18	1214.00	17	Geisum-W-2	27.68	33.66	122.44	2954.43	32	Fesyan-B-1X	27.66	33.75	79.38	1629.00
3	EEMM—28	27.49	33.62	80.78	1305.15	18	Malak-1	27.23	33.66	142.44	3692.96	33	Rabeh--2	27.22	33.75	105.78	1958.64
4	FE-87	27.48	33.63	73.68	1436.00	19	S.Malak--1x	27.23	33.67	143.00	3415.28	34	Rabeh--4	27.22	33.75	94.67	1933.96
5	EEMM-18	27.49	33.63	83.00	1367.03	20	Hudhud--1	27.28	33.67	80.78	1645.62	35	Abu-marwa-n-1	27.21	33.77	100.22	1965.96
6	EEMM-21	27.49	33.63	76.89	1265.53	21	Gemsa-Alpha-1	27.58	33.69	121.56	3194.00	36	Abu-Marwa-N-1	27.21	33.77	100.22	1965.96
7	EEMM-3	27.46	33.63	79.11	1694.99	22	NW-Tanan--1	27.27	33.69	115.22	2552.70	37	Felefel-1	27.32	33.81	81.33	1358.49
8	EEMM-16	27.46	33.63	78.00	1264.92	23	S.-Geisum-3	27.65	33.70	78.86	1665.00	38	Felfel-2	27.32	33.82	64.55	975.00
9	EEMM-20	27.46	33.63	73.56	1355.45	24	Tawila-W-3	27.58	33.71	127.53	3125.00	39	Gubal-East-1X	27.68	33.84	123.64	2613.00
10	EEMM-24	27.46	33.63	80.78	1775.46	25	Abu-Milka-1	27.33	33.72	138.27	3150.00	40	UM-GAWISH--1	27.13	33.84	89.11	1679.45
11	EEMM-8	27.45	33.63	103.00	1224.38	26	Abu-Milka--1	27.21	33.72	111.89	3150.11	41	Estakoza-1	27.43	33.89	87.44	1602.64
12	EEMM-8A	27.48	33.63	83.00	1719.99	27	Tawila-W-2	27.56	33.73	180.51	4275.00	42	Hareed--2	27.35	33.93	97.44	2662.43
13	EEMM-17	27.46	33.63	78.00	1371.60	28	Wadi-Elsahl-N1	27.20	33.72	120.22	2819.40	43	Hareed--1-ST1	27.35	33.93	93.00	2065.02
14	EEMM-19	27.46	33.63	93.00	1462.43	29	Tawila-N-1	27.59	33.73	121.58	3129.00	44	GH-451	27.69	33.94	163.32	2798.00
15	EEMM-25	27.45	33.63	82.44	1334.11	30	Fg-88-11	27.68	33.73	78.60	1196.00						

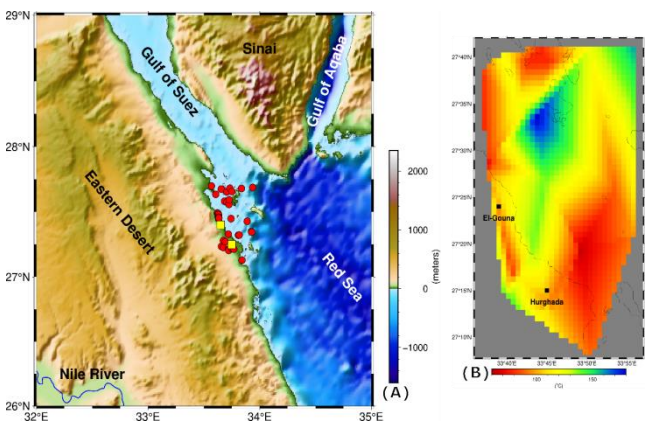

Figure 9. (A) DEM shows the temperatures represented by the red dots, and (B) the BHT interpolated from A.

3.2. Data Approach

3.2.1. Geothermal Gradient

We grouped the 44 onshore and offshore wells and its average depth and temperature into 8 slices from top to bottom ascending in the direction of temperature gradient increase per 100m (**Figure 2**) and then we took each layer and calculated its own average gradient to find out the layer at which the temperature gradient is maximum and hence know it's depth (Table 1) we also made a graph to show the gradient variations from one slice to another (**Figure 3**).

3.2.2. Temperature Relations with the Data

We interpolated the data from each model to determine which is more connected to BHT and the temperature gradient distribution over the study area (**Figures 4A, B&C**).

4. Conclusion

The geothermal potential of the Hurghada region in the southern Gulf of Suez was investigated to address the problem of underutilized renewable energy resources in Egypt, particularly in tectonically active settings. Analysis of Bottom Hole Temperature (BHT) data from 44 wells, stratigraphically organized into eight depth intervals, revealed a consistent but nonlinear temperature increase with depth, influenced by structural controls such as faulting and crustal thinning. Key findings include the identification of elevated geothermal gradients, particularly in the fourth and fifth isothermal layers, correlated with shallow Curie temperature depths and high BHT values, highlighting zones of enhanced geothermal potential. These results demonstrate that the region's unique

tectonic evolution, marked by Oligocene–Miocene rifting, has created favorable conditions for geothermal energy accumulation, The implications of these findings are significant for Egypt's renewable energy strategy. The Hurghada area presents a scientifically validated opportunity for geothermal resource development, offering the potential to diversify Egypt's energy sources, reduce carbon emissions, and enhance energy security. Furthermore, the integrated use of geological, magnetic, and gravity datasets has proven essential for identifying and characterizing geothermal hotspots with greater precision.

Future work should focus on detailed geothermal reservoir characterization, including exploratory drilling, thermal conductivity measurements, and the development of pilot geothermal projects to assess economic viability. Additionally, integrating 3D geomechanical modeling and advanced geophysical imaging could refine subsurface predictions and further reduce exploration risk. In conclusion, this study positions the Hurghada region as a prime target for geothermal energy exploitation in Egypt. Unlocking this resource could serve as a critical step toward achieving national sustainability goals and transitioning to a cleaner, more resilient energy future.

5. Acknowledgements

The authors thank all the persons who contributed in this work, directly or indirectly with data availability. All cited through the main text.

6. Conflict of interest

The authors imply that there is no conflict of interest with any authors or others. Also, this manuscript has not been published and is not under consideration for publication elsewhere. The authors have no relevant financial or non-financial interests to disclose.

References

[1] Abd El Aziz, E.A.A.E.; Gomaa, M.M. Electrical properties of sedimentary microfacies and depositional environment deduced from core analysis of the syn-rift sediments, Northwestern shore of Gulf of Suez, Egypt. J. Petrol. Explor. Prod. Technol. 2022, 12(11), 2915–2936

[2] Gaber, G. M.; Kotb, A.; Saleh, S. Review of the Geothermal Resources in the Central Eastern Desert of Egypt: 2000-2024. Adv. Basic Appl. Sci. 2024, 3(1), 47-51.

[3] Bekhit, A.M.; Sobh, M.; Abdel Zaher, M.; Abdel Fattah, T.; Diab, A.I. Crustal thickness variations beneath Egypt through gravity inversion and forward modeling: linking surface thermal anomalies and Moho topography. *Prog. Earth Planet. Sci. 2024*, *11*(1), 39.

[4] Gaber, G.M.; Saleh, S.; Toni, M. Crustal thickness and structural pattern evaluation of Sinai Peninsula using three-dimensional density modeling with aeromagnetic and earthquake data. *Acta Geophysica. 2022*, *70*(2), 639–657.

[5] Abdelwahed, M.F.; El-Khrepy, S.; Qaddah, A. Three-dimensional structure of Conrad and Moho discontinuities in Egypt. *J. Afr. Earth Sci.* 2013, *85*, 87–102.

[6] Tian, J.; Pang, Z.; Liao, D.; Zhou, X. Fluid geochemistry and its implications on the role of deep faults in the genesis of high temperature systems in the eastern edge of the Qinghai Tibet Plateau. *Appl. Geochem. 2021*, *131*, 105036

[7] Joffe, S.; Garfunkel, Z. Plate kinematics of the circum Red Sea: a re-evaluation. *Tectonophysics. 1987*, *141*(1–3), 5–22.

[8] Bosworth, W.; Taviani, M. Late Quaternary reorientation of stress field and extension direction in the southern Gulf of Suez, Egypt: Evidence from uplifted coral terraces, mesoscopic fault arrays, and borehole breakouts. *Tectonics. 1996*, *15*(4), 791–802.

[9] Moustafa, A.R.; Khalil, S.M. Structural setting and tectonic evolution of the Gulf of Suez, NW Red Sea, and Gulf of Aqaba rift systems. *The Geology of Egypt. 2020*, 295–342.

[10] Abdel Zaher, M.; El-Qady, G.; Elbarbary, S. Geothermal potentiality of Egypt: review and updated status. *The Phanerozoic Geology and Natural Resources of Egypt*, 2023b, 637–648.

[11] Said, R. *The geology of Egypt*. Routledge. 2017.

[12] Abd El Naby, A.; Abd-Elaziz, W.; Aal, M.H.A. Biostratigraphy and seismic data analysis to detect the sequence stratigraphic depositional environment of the Miocene succession: Gulf of Suez (Egypt). *Swiss J. Geosci.* 2017, *110*, 777–791.

[13] Abdel Zaher, M.; Elbarbary, S.; Mohammad, A.T.; Saibi, H.; Matsumoto, M.; Nishijima, J.; Fujimitsu, Y. Numerical simulation of heat and mass transfer in the Hurghada–El Gouna geothermal field in Egypt. *Geothermics. 2023a*, *115*, 102820.

[14] Segev, A.; Avni, Y.; Shahar, J.; Wald, R. Late Oligocene and Miocene different seaways to the Red Sea–Gulf of Suez rift and the Gulf of Aqaba–Dead Sea basins. *Earth-Sci. Rev.* 2017, 171, 196–219

[15] Patton, T.L.; Moustafa, A.R.; Nelson, R.A.; Abdine, S.A. Tectonic evolution and structural setting of the Suez Rift. 1994.

[16] Bekhit, A.M.; Sobh, M.; Abdel Zaher, M.; Abdel Fattah, Th.; Diab, A.I. Predicting terrestrial heat flow in Egypt using random forest regression: a machine learning approach. Geothermal Energy 2025, 13, 18.

[17] Amante, C.; Eakins, B.W. ETOPO1 arc-minute global relief model: procedures, data sources and analysis. 2019.

[18] Zingerle, P.; Pail, R.; Gruber, T.; Oikonomidou, X. The combined global gravity field model XGM2019e. *J. Geod. 2020*, *94*(7), 66.

[19] Uieda, L.; Barbosa, V.C.; Braitenberg, C. Tesseroids: Forward-modeling gravitational fields in spherical coordinates. *Geophysics. 2016*, *81*(5), F41–F48.

[20] Laske, G.; Masters, G.; Ma, Z.; Pasyanos, M. Update on CRUST1.0—A 1-degree global model of Earth's crust. In *Geophys. Res. Abstr. 2013*, *15*(15), 2658.

[21] Saleh, S.; Jahr, T.; Jentzsch, G.; Saleh, A.; Abou Ashour, N.M. Crustal evaluation of the northern Red Sea rift and Gulf of Suez, Egypt from geophysical data: 3-dimensional modeling. *J. Afr. Earth Sci. 2006*, *45*(3), 257–278.
[22] Meyer, B.; Chulliat, A.; Saltus, R. Derivation and error analysis of the earth magnetic anomaly grid at 2 arc min resolution version 3 (EMAG2v3). *Geochem. Geophys. Geosyst. 2017*, *18*(12), 4522–4537.
[23] Li, C.F.; Lu, Y.; Wang, J. A global reference model of Curie-point depths based on EMAG2. *Sci. Rep. 2017*, *7*(1), 45129.
[24] Sayed, M.; Sobh, M.; Saleh, S.; Othman, A.; Elmahmoudi, A.3D crustal density modeling of Egypt using GOCE satellite gravity data and seismic integration. *Earthquake Sci. 2024.*
[25] Waples, D.W.; Pacheco, J.; Vera, A. A method for correcting log-derived temperatures in deep wells, calibrated in the Gulf of Mexico. *Petrol. Geosci. 2004*, *10*(3), 239–245.